Journal of the Society of Automotive Engineers Malaysia
Volume 6, Issue 1, pp 46-64, January 2022
e-ISSN 2550-2239 & ISSN 2600-8092

Forward Collision Prevention System for Two-wheeler Bike Using Berkeley Algorithm-Based PID Control

O. Z. Zhao[1], **V. R. Aparow**[1]*, Z. M. Jawi[2] and K. A. Abu Kassim[2]

[1] Automated Vehicle Engineering System (AVES) Group, Electrical & Electronics Engineering Dep., Fac. of Science and Eng., University of Nottingham Malaysia, Jalan Broga, 43500, Semenyih, Selangor, Malaysia.
[2] Malaysian Institute of Road Safety Research (MIROS), 43000 Kajang, Selangor, Malaysia

*Corresponding author: Vimal.Rau@nottingham.edu.my

ORIGINAL ARTICLE *Open Access*

Article History:

Received
15 Sep 2021

Accepted
7 Dec 2021

Available online
1 Jan 2022

ABSTRACT – *This manuscript summarizes the development of a Forward Collision Prevention (FCP) system for two-wheeler bike dynamics to prevent a frontal collision. A four Degree of Freedom (4-DOF) longitudinal bike model was derived and integrated with the magic tire model. Several handling tests such as the full-throttle acceleration and braking test are performed to validate the developed model. Then the model is then used as a plant to develop the Forward Collision Prevention (FCP) system. The throttle and brake control models were developed to control the throttle level and brake torque of the bike model. A PID controller is implemented with the Berkeley algorithm to overcome the nonlinearity of the entire model. The developed controller can maintain a safe distance of 60m to 70m between the leading vehicle and the two-wheeler bike to prevent a forward collision.*

KEYWORDS: Forward collision prevention, two-wheeler bike, PID controller, Berkeley algorithm

Journal homepage: www.jsaem.my

1. INTRODUCTION

Various advanced safety driving assistance systems have become more common in four-wheelers to help drivers on a daily driving basis and improve driving; however, most systems are still new for two-wheelers (Turner & Higgins, 2013; Biral et al., 2010). Advanced safety technologies such as Forward Collision Warning (FCW), Adaptive Cruise Control (ACC), and Lane Keeping Assist System (LKAS) are not only found in high-end vehicles but also in lower or entry-level vehicles (Chen et al., 2019; Zhang et al., 2020; Zhang et al., 2021). The goal of developing a fully functional autonomous vehicle is getting closer for engineers to develop a perfect working algorithm and advanced system to improve the quality of driving (Zhang et al., 2020; Zhang et al., 2021). The evolution of two-wheelers is similar to passenger vehicles, but they are much slower compared to technological development for passenger vehicles (Savino et al., 2020). Thus, the possibility of road accidents involving motorcyclists is still high in most developing countries, especially in the Asian region (Abdul Manan et al., 2018).

Among various types of accidents on road, forward collision occurs the most and has the highest fatal rates for two-wheeler vehicles. Research from the Malaysian Institute of Road Safety and Research (MIROS) indicates a potentially serious problem with motorcyclist safety, given that the motorcyclist demographic makes up 25% of all fatalities in road accidents. The MIROS data is relatively close to the Asian average, with motorcycles making up 47% of all registered vehicles in Asia. In the same vein, 59% of all fatalities stemming from road accidents are attributed to motorcyclists, which is once again close to Malaysia's average (Abdul Manan et al., 2018, MIROS, 2018). Therefore, these statistics are of importance to the study because two-wheeler is dominant in the majority of Asia's developing nations. Unfortunately, this mode of transport leaves the rider at significant risk of encountering an accident, with head injuries a particularly prevalent aftereffect. Accidents have commonly occurred as a result of loss of control after a collision with an object such as a vehicle. MIROS reports revealed that the economic impact of the fatalities from motorcycle crashes is staggeringly high, at an average of MYR

6.45 billion a year since 2010 (Abdul Manan et al., 2018, MIROS, 2018).

To minimize road accidents involving motorcyclists, a lot of motorbike manufacturers focused on applying technology called the Forward Collision Warning (FCW) system. Research works focusing on FCW systems have been developed by vehicle manufacturers such as Mercedes and Volvo and applied in most four-wheeler vehicles (Biral et al., 2010, Savino et al., 2020). FCW is designed to provide warning to the driver during situations critical conditions to avoid frontal collision (Dagan et al., 2004; Bloecher et al., 2009; Cicchino, 2017). Previous research works show that the main causes of rear-end collisions are due to drivers not paying attention while driving (Zador et al., 2000; Bonci et al., 2016; Wang et al., 2016). To attract drivers' attention to their riding task and reduce the risk of rear-end collision, the FCW system should be implemented in vehicles. The main criteria for an FCW system to work is to determine the safety distance between two vehicles and provide a warning to the drivers (Sharp et al., 2004; Bonci et al., 2016; Barbagallo et al., 2016). Usually, the safety distance is measured as the summation of the vehicle's minimum braking distance and the minimum headway distance between vehicles (Bonci et al., 2016; Bonci et al., 2017; Bonci et al., 2018).

Radar sensors are commonly used in FCW systems, as radar sensors have a high level of accuracy in detecting objects, it is robust and capable to sense a wide range. But it does come with a high price tag (Bloecher et al., 2009). A lower-cost camera vision sensor is also used in the FCW system as camera sensors are usually used to detect lanes, cars, and pedestrians in a shorter-range distance (Dagan et al., 2004; Milanés et al., 2012). For the FCW system to work, there are a few parameters that need to be considered in the technological development of motorcycles. Firstly, the velocity and the maximum deceleration of a motorcyclist, the minimum braking distance of a vehicle, and the minimum headway distance to be set (Kusano & Gabler, 2012; Chen et al., 2013). The FCW system will evaluate the level of risk of potential frontal collision where there are three levels of risk: low, medium, and high. Each level of risk will have different feedback to the rider where higher risk will provide a louder audible sound and brighter display to the rider to catch the rider's attention about the possible upcoming frontal collision. According to studies for two-wheeler bikes, studies examining collision warning systems reported high levels of detection but noted limitations with existing technology in terms of real-time implementation and timing. An advanced version of the FCW system such as the Adaptive Cruise Control (ACC) system is required for motorcyclists to help the riders to maintain a safety distance automatically and the velocity of the bike from the front obstacle.

Based on the previous shortcomings, Forward Collision Prevention (FCP) system is developed in this study for the motorcyclist based on Adaptive Cruise Control from vehicle technology. This technology is designed to support the motorcyclist to not only provide warning to the riders but help the rider to reduce the longitudinal velocity to avoid any frontal collision. The system aids the rider in not hitting the front proceeding vehicle by activating the FCP if the rider does not have enough time to react if the front proceeding vehicle suddenly decelerates or stops. The FCP is designed by using the Berkeley algorithm, which is based on the Mazda algorithm that has been improved (Zhang et al., 2020). The algorithm provides critical alarm distance response which is used as the desired input to reduce the frontal collision using the PID controller. To evaluate the performance of the Berkeley algorithm-based PID control, a 4-DOF two-wheeler bike model is developed in this study which consists of the dynamic model, tire model, powertrain, and brake model. Three types of different driving conditions are used to evaluate the performance of the two-wheeler bike model equipped with Berkeley algorithm-based PID control design.

The paper is organized as follows: The first section explains the introduction and related works on the Forward Collision Warning system and its application for motorcyclists. The second section explained the development of a 4-DOF two-wheeler bike model using various subsystem models. Meanwhile, the third section briefly discussed the vehicle longitudinal model which is used as the leading vehicle for testing the Forward Collision Prevention system. The next section discusses controller development using the Berkeley algorithm and PID controller. The fifth section explains the simulation results using three different testing scenarios and finally is the conclusion for this paper.

2. BIKE MODELLING

In this section, the mathematical equation of the bike model is derived. The equations will be then modeled in SIMULINK to form a complete mathematical model of a two-wheeler bike. The simulation result of the mathematical model will then be verified with the results from BikeSim. The expected outcome will be the mathematical model results following the trend result of the BikeSim simulation. The response of the two-wheeler bike model is compared in terms of two-wheeler bike velocity.

2.1 Bike Longitudinal Model

For the design of the bike model, the essential characteristics are the longitudinal velocity of the bike and the rotational velocities of the wheels. Hence, a half-car model will be used as a reference to develop the 4-DOF bike model. The longitudinal model also includes the powertrain model and the brake model.

2.1.1 Longitudinal Forces

In the project, the development of the bike model will be based on the half-car vehicle longitudinal model. The main primary force of interest is the longitudinal force of the bike model which acts along the x-axis of the bike. A normal force is proportional along the z-axis at both the rear and front tires as shown in Figure 1.

$$F_{x,fi} = \mu F_{z,fi} \quad (1)$$

$$F_{x,ri} = \mu F_{z,ri} \quad (2)$$

Where,

i = l for the left wheel and r for the right wheel
$F_{x,fi}$ = longitudinal force acting on front left and right tire
$F_{x,ri}$ = longitudinal force acting on rear left and right tire
$F_{z,fi}$ = normal force acting on front left and right tire
$F_{z,fi}$ = normal force acting on rear left and right tire

The total longitudinal force is the sum of the front and rear longitudinal force acting on the two-wheeler bike model:

$$F_{X_{total}} = 2F_{x,fi} + 2F_{x,ri} \quad (3)$$

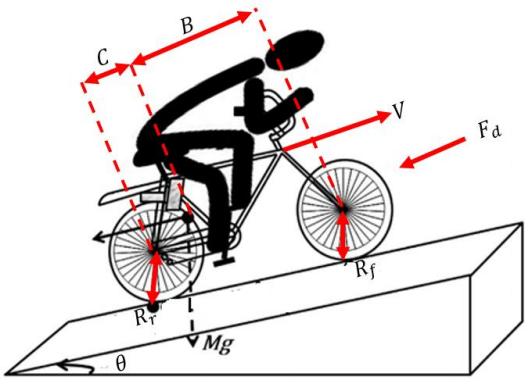

FIGURE 1: Schematic diagram of two-wheeler bike

From Figure 1, the total forces acting on the two-wheeler bike's mass can be expressed in equation (4) as follow:

$$\frac{dV}{dt} = \frac{-F_{X_{total}} + g \sin\theta + F_d}{M} \quad (4)$$

Where,
$F_{X_{total}}$ = total longitudinal force acting on two-wheeler bike body
F_d = drag force
θ = angle of the slope
g = gravitational force

2.1.2 Drag Forces

From equation (4), the drag force, F_d is dependent on the two-wheeler bike's velocity. It acts as a limiter to the two-wheeler bike's maximum velocity. The total drag force is the summation of all resistive force to the two-wheeler bike which is the aerodynamic force, F_a, and the rolling resistive force, F_r.

$$F_d = F_a + F_r \quad (5)$$

$$F_a = \frac{1}{2}\rho A C_d (V^2) \quad (6)$$

$$F_r = mgC_r(V) \quad (7)$$

Where,

C_r = rolling resistance coefficient
A = frontal area of the two-wheeler bike
C_d = aerodynamic drag coefficient
ρ = density of air which is 1.23 kg/m^3

2.1.3 Load Distribution

The load distribution for the front and rear wheels can be found in equation (4). The load distribution of the two-wheeler bike is the normal force that is acting on the wheel of the two-wheeler bike. The static load distribution is the grade angle and a function of two-wheeler bike geometry and can be obtained by adding up the forces of both wheels. Whenever the two-wheeler bike accelerates or brakes, the load of the two-wheeler bike is transferred to both wheels based on dynamic load distribution.

$$F_{z,fi} = mg\left[\frac{C}{L}cos(\theta) + \frac{H}{L}sin(\theta)\right] - m\left(\frac{dV}{dt}\right)\frac{H}{L} \quad (8)$$

$$F_{z,ri} = mg\left[\frac{B}{L}cos(\theta) + \frac{H}{L}sin(\theta)\right] - m\left(\frac{dV}{dt}\right)\frac{H}{L} \quad (9)$$

2.1.4 Longitudinal Slip Model

In the bike model, the effect of friction coupling is accounted for in the longitudinal slip model as expressed in equations (10) and (11):

$$\lambda_{fi} = \frac{V - \omega_{fi}R}{\max(V, \omega_{fi})} \quad (10)$$

$$\lambda_{ri} = \frac{V - \omega_{ri}R}{\max(V, \omega_{ri})} \quad (11)$$

Where,

ω_{fi} = front wheel angular velocity
ω_{ri} = rear wheel angular velocity
λ_{fi} = front wheel longitudinal slip
λ_{ri} = rear wheel longitudinal slip

2.1.5 Tire Model

Other studies showed that there are several characteristics of friction/slip between the tire and road surface (Aparow et al., 2013; Ahmad et al., 2014). These characteristics can then be categorized into four different types of road conditions as shown in Table 1. Meanwhile, Figure 2 shows the friction vs slip characteristic using four different road conditions.

TABLE 1: Friction/slip characteristics for all four types of road conditions (Aparow et al., 2013)

Road Condition	Characteristics
Normal/Dry	The road is dry and approaches maximum traction condition.
Raining/Wet	Overall traction condition is reduced to 20% from the normal road condition.
Snow	Road surface appears to be unpacked snow with traction reduced by 65%.
Ice	Packed froze snow and black ice lie on the road surface. The maximum traction is reduced by 95% and can considered to be a very dangerous road condition.

At this point, the Pacejka magic formula can step in to simulate the slip/friction characteristic of the tire models. The formula is implemented in equations (12) and (13).

$$\mu_{fi}(\lambda) = D\ sin\left\{C\ arctan\left(B\lambda_{fi} - E\left(B\lambda_{fi} - arctan\left(B\lambda_{fi}\right)\right)\right)\right\} \quad (12)$$

$$\mu_{ri}(\lambda) = D\ sin\left\{C\ arctan\left(B\lambda_{ri} - E\left(B\lambda_{ri} - arctan(B\lambda_{ri})\right)\right)\right\} \quad (13)$$

The coefficients B, C, D and E are the factors in the equation as follows:

- B = stiffness factor,
- C = shape factor,
- D = peak factor,
- E = curvature factor.

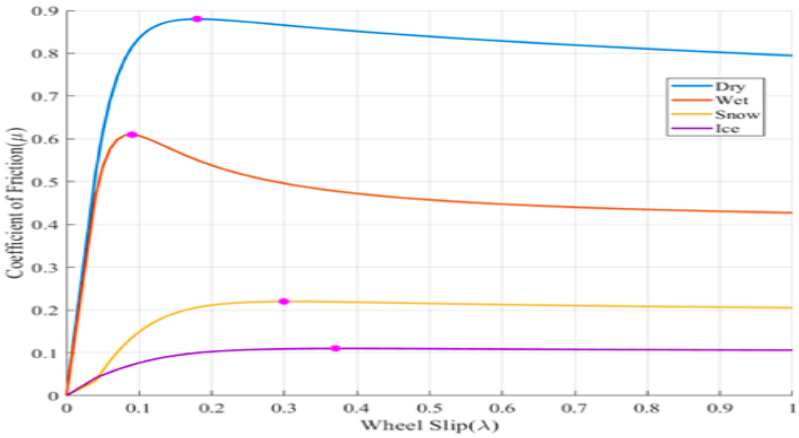

FIGURE 2: Friction/slip characteristic curve for all road conditions

The values of these factors vary with different types of road conditions which are shown in Table 2.

TABLE 2: Pacejka tire model parameters (Aparow et al., 2013)

Pacejka Coefficients				
Surface	*B1*	*C1*	*D*	*E*
Dry surface	10	1.9	1	0.97
Wet surface	12	2.3	0.82	1
Snow surface	5	2	0.3	1
Icy surface	4	2	0.1	1

2.1.6 Wheel Dynamic Equations

The sum of the torque acting on the torque forms the equations of the motions of the wheel velocity based on Figure 3:

$$\omega_{fi} = \frac{\tau_{e_{fi}} + \tau_{r_{fi}} - \tau_{b_{fi}} - \tau_{d_{fi}}}{J_{fi}} \quad (14)$$

$$\omega_{ri} = \frac{\tau_{e_{ri}} + \tau_{r_{ri}} - \tau_{b_{ri}} - \tau_{d_{ri}}}{J_{ri}} \quad (15)$$

where τ_(e_fi) and τ_(e_ri) are the torques delivered by the engine to each wheel and τ_(b_fi), and τ_(b_ri) are the brake torques applied to each wheel during braking input. Since this bike is a two-wheeler bike model, the engine torque for the front wheel is assumed to be zero.

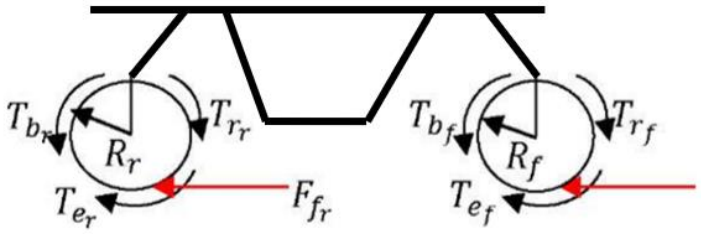

FIGURE 3: Torques on the bike wheel

2.2 Power Train Model

The engine of a two-wheeler bike is a combination of multiple subsystems such as the gearbox, torque converter, and final drive differential. The powertrain transfers the engine torque to the wheels whenever the bike accelerates or decelerates (brake). The engine torque is transferred only to the rear wheel as the bike is a rear-wheel-drive model.

2.2.1 Engine Torque Curve

For a typical small scooter, the 250cc engine can provide the power of 24kW and has a peak engine torque of 23.97Nm at 7500 RPM. The engine model is developed mathematically based on data obtained from BikeSim engine parameters using SIMULINK. The modeling of the curve is done through the “Lookup Table” function in SIMULINK. Figure 4 below shows the Engine RPM vs Engine torque graph at different throttle levels.

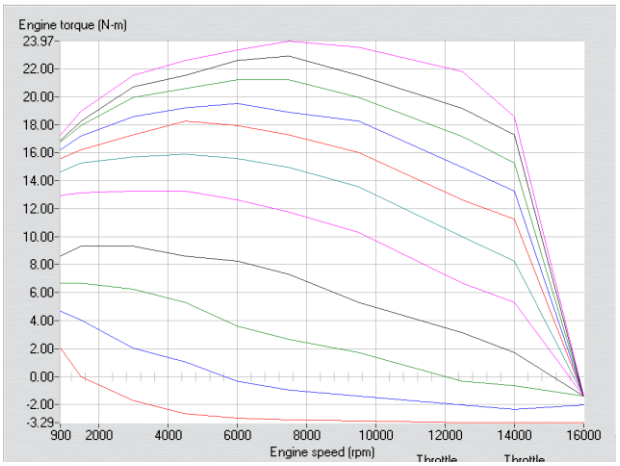

FIGURE 4: Engine torque (N-m) vs. engine velocity (RPM) curve at different throttle levels

2.2.2 Gearbox Model

The gearbox model for the scooter is a 5-speed automatic transmission gearbox. An automatic transmission gearbox is a system that utilizes shift logic, where it produces a mapping logic that shifts the gear number based on the throttle position and transmission speed. From Figures 5 and 6, the shift logic shifts the gear accordingly to the engine transmission speed and the throttle position. From Figure 5, the upshift logic occurs at the throttle ranges from 10% and 20% to 85% as the transmission speed increases. On the other hand, the downshift logic occurs at the throttle range of around 25% and 65% as the transmission speed decreases. These data are plotted with the 'lookup table' function in SIMULINK and use the state selection function to develop the overall shift logic of the gearbox. Hence, based on Figures 5 and 6 the following expression are found.

$$\text{Upshift logic} = \begin{cases} \text{if} & \mu_t \leq 10 - 20\% & \text{transmission speed is maintained} \\ \text{if} & 30\% < \mu_t \leq 85\% & \text{transmission speed is increased} \\ \text{if} & \mu_t > 85\% & \text{transmission speed maintain and gear increase} \end{cases} \quad (16)$$

$$\text{Downshift logic} = \begin{cases} \text{if} & \mu_t \leq 25\% & \text{transmission speed maintain and gear is decreased} \\ \text{if} & 25\% < \mu_t \leq 65\% & \text{transmission speed is decreased} \\ \text{if} & \mu_t > 65\% & \text{transmission speed is maintained} \end{cases} \quad (17)$$

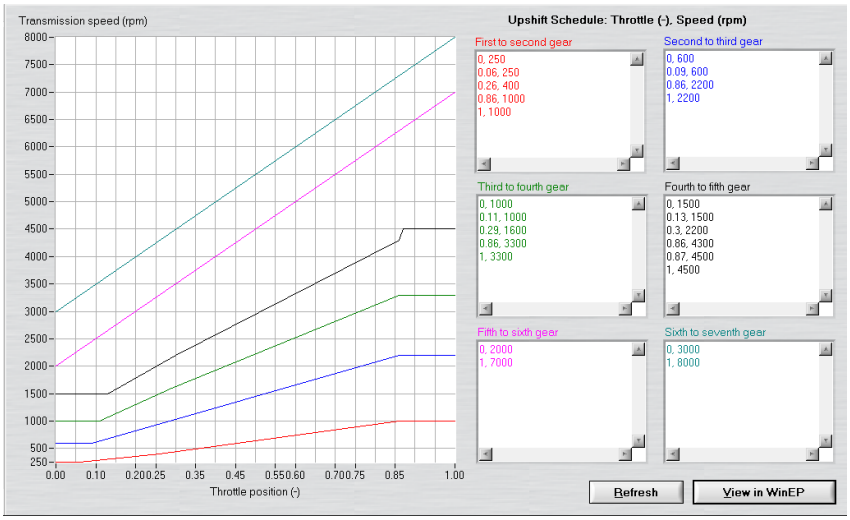

FIGURE 5: Upshift logic for the gearbox (pink line and light blue line neglected)

The upshift and downshift of the gearbox depending on the acceleration and deceleration of the bike. Whenever the bike accelerates or decelerates, the gear ratio will increase or decrease in reference to the upshift or downshift logic. Therefore, the expression below concludes the mechanism of the automatic transmission gearbox.

$$\text{Gear Shifting} = \begin{cases} \text{if} & \mu_t \leq 25\% & \text{bike decelerate so gear shift down} \\ \text{if} & \mu_t > 85\% & \text{bike accelerate so gear shift up} \\ \text{else} & - & \text{bike maintain speed and so gear is maintained} \end{cases} \quad (18)$$

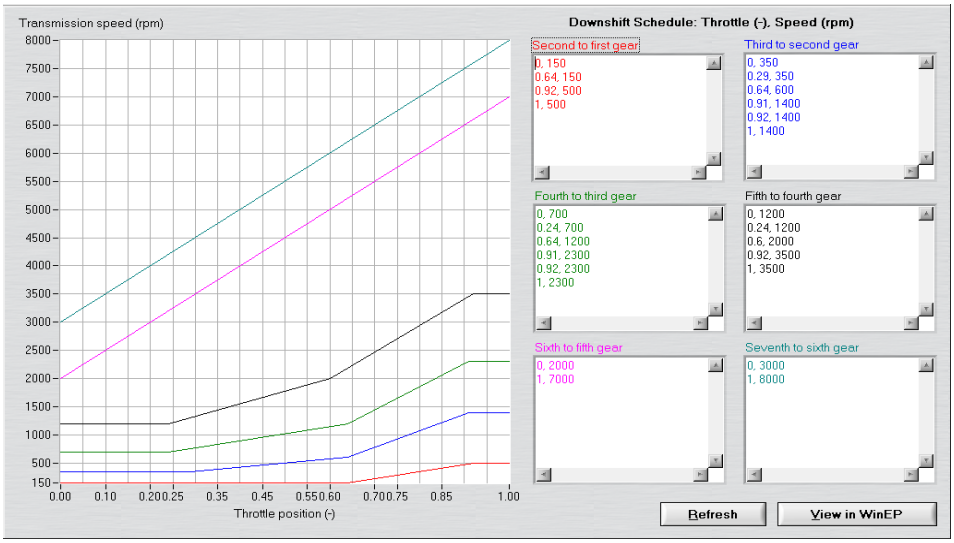

FIGURE 6: Downshift logic for the gearbox (pink line and light blue line neglected)

Figure 7 shows the threshold calculation function for upshifting and downshifting logic. Meanwhile, Figure 8 shows the gearbox model developed using the SIMULINK function blocks. The input to the function is throttle position and transmission speed, the output is the gear number.

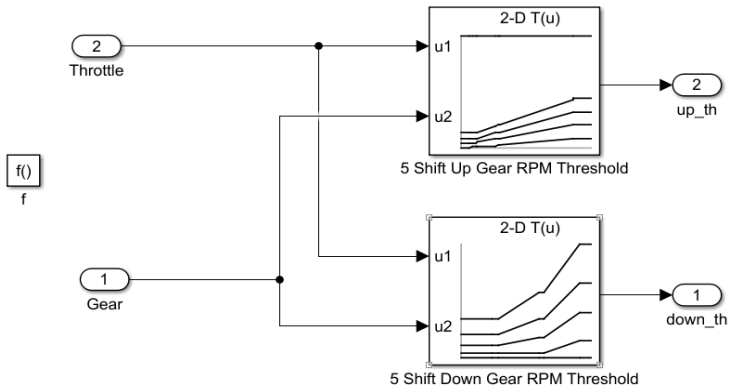

FIGURE 7: Threshold calculation of the gearbox model

In this SIMULINK function, there are two states which are the gear state and the selection state. The gear state is the gear number of the bike model, and each gear has its respective gear ratio. The selection state act as a controller to choose the gear number, the selection state uses ‘down_th’ and ‘up_th’ to trigger the changing of gear state. The ‘down_th’ and ‘up_th’ are the threshold value for changing gear numbers, and the respective threshold value can be found in Figures 5 and 6. As shown in Figure 8, whenever the transmission RPM exceeds the threshold value for both the upshift and downshift limit, the selection state will trigger the downshifting or upshifting function block to change the

gear number. If the transmission RPM maintains within the threshold value, the selection state will stay at a steady state block and the bike model maintains its current gear number.

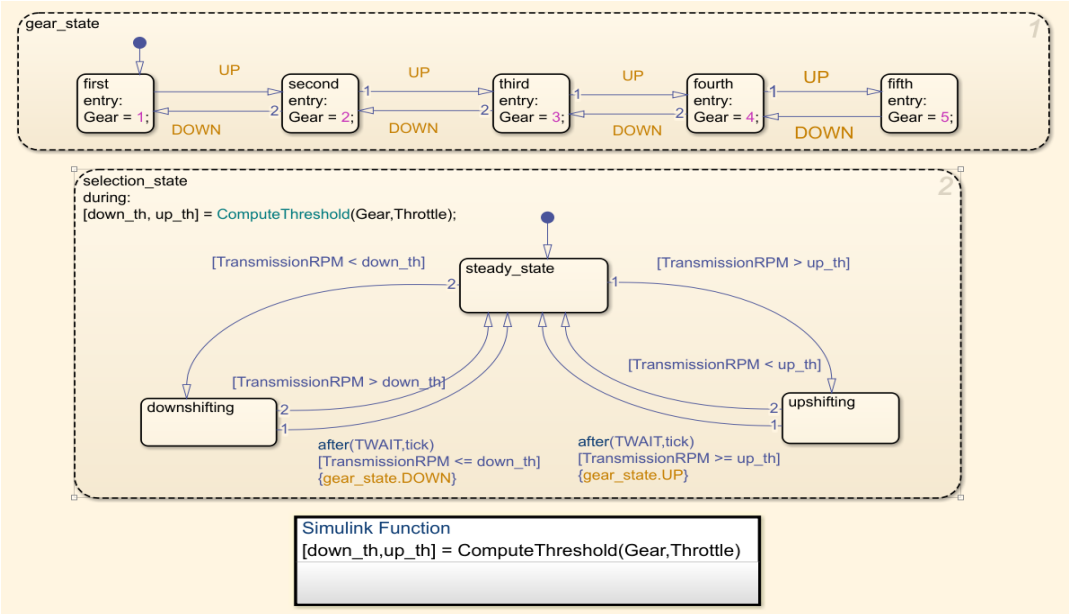

FIGURE 8: Gearbox model for two-wheeler bike model

2.2.3 Bike Brake Model

The brakes are mainly described by their mechanical properties and the hydraulics feeding by the brakes. The rider inputs the forces to the brake lever on the handle and the foot lever. There are two master cylinders connected with each booster for the front and rear brakes. The master cylinder pressure can be calculated as follow:

$$Master\ Cylinder\ Pressure = \frac{Booster\ Force}{Master\ Cylinder\ Area} \tag{19}$$

Both master cylinders have a total surface area of 198.5mm2 and the front brake lever ratio is six while the rear brake has a lever ratio of three. The pressure will then be delivered to the wheel cylinder at unity gain. The brake output torque can be obtained by multiplying the wheel cylinder pressure with the wheel cylinder area, pad friction coefficient, respective lever ratio, and the effective disc radius as shown in the equation below.

$$Brake\ Torque = Wheel\ Cylinder\ Pressure \times Wheel\ Cylinder\ Area \times Lever\ Ratio \times Pad\ Friction\ Coefficient \times Disc\ Radius$$

2.3 Overview of the Bike Model

As mentioned above, the complete bike model is shown in Figure 9, which is designed based on the vehicle body dynamic model, the load distribution model, the tire model, the longitudinal slip model, the wheel dynamic model, and the powertrain model.

2.4 Simulation Parameters

Table 3 shows the parameters of the bike longitudinal model in simulation. These parameters are obtained based on the small scooter with a 250cc engine. Meanwhile, Table 4 shows the gear ratio of the bike's automatic transmission gearbox.

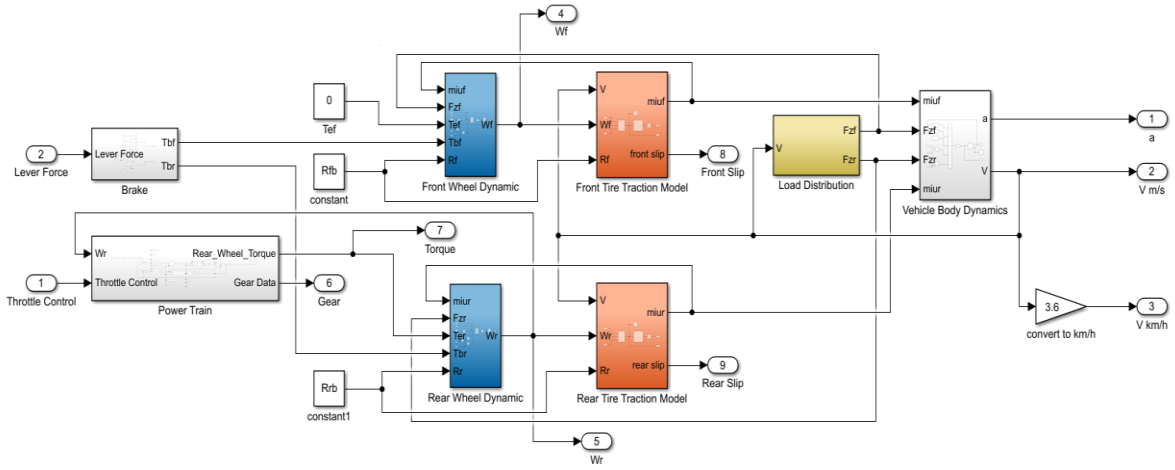

FIGURE 9: Schematic diagram of the complete bike model

TABLE 3: Parameters used in the simulation of the vehicle longitudinal model

Parameter	Symbol	Value
Bike Mass	M_b	230 kg
Front Area of Bike	A_b	0.6 m^2
Front Wheelbase	B_b	0.4 m
Rear Wheelbase	C_b	0.778 m
Total Wheelbase	L_b	1.178 m
Height of Bike	H_b	0.4 m
Wheel Radius	R_b	0.2 m
Front Moment of Inertia	J_{fb}	0.484 kg/m^2
Rear Moment of Inertia	J_{rb}	0.638 kg/m^2
Gravitational Constant	g	9.81 m/s^{-2}
Density of Air	Roh	1.23 kg/m^3
Aerodynamic Drag Coefficient	C_d	0.52
Rolling Resistance Coefficient	C_r	0.0003
Viscous Friction Coefficient	C_{fi}	0.1 Nm/rad s^{-1}
Master Brake Cylinder Surface Area	Mc_{ab}	198.5 mm^2
Front Brake Cylinder Surface Area	Wc_{fb}	2050 mm^2
Rear Brake Cylinder Surface Area	Wc_{rb}	2300 mm^2
Front Brake Disc Radius	D_{fb}	0.148 m^2
Rear Brake Disc Radius	D_{rb}	0.098 m^2
Front Brake Lever Ratio	L_{fb}	6
Rear Brake Lever Ratio	L_{rb}	3
Brake Pad Coefficient	C_{bb}	0.4

TABLE 4: Gear ratio used in the simulation of vehicle longitudinal model

Parameter	Ratio
Final drive ratio	2.89
1st gear	2.7
2nd gear	1.8
3rd gear	1.4
4th gear	1.12
5th gear	0.95

2.5 Simulation Result

Figure 10 shows the throttle setting and the brake setting of the bike model in the SIMULINK simulation. The bike model is tested with the step function of the throttle and brakes input. The bike is at rest from t = 0s to t = 5s, the bike is then accelerated at full throttle to t = 60s. At t = 60s, the throttle is dropped to 0 and 100N brake force is applied at the pedal. Figures 10 and 11 show the velocity, front-wheel velocity, and rear-wheel velocity of the bike model. From Figure 11, the bike model achieves a top velocity of 93 km/h, a rear-wheel velocity of 108 km/h, and a front-wheel velocity of 92 km/h. There is an inconsistency in the result from the velocity of the wheels as the rear wheel velocity is 15 km/h faster than the bike velocity. This is mainly because the engine torque is directly connected to the rear wheel which produced higher velocity than the front wheel. The front wheel is reduced due to mechanical transmission from the rear wheel to the front wheel. Meanwhile, the bike velocity is lowered compared to the rear wheel velocity because of aerodynamic and rolling resistance which has been included in equation (5).

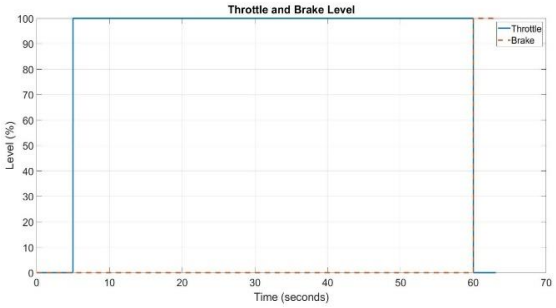

FIGURE 10: Throttle and brake setting

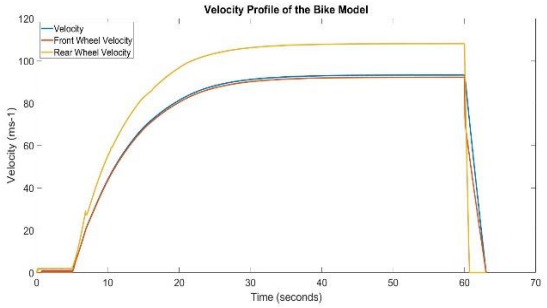

FIGURE 11: Bike Velocity Profile

3. LEADING VEHICLE LONGITUDINAL MODEL

To conduct the simulation analysis for the two-wheeler bike model, a leading vehicle model is required in this analysis. Therefore, in this study, the 5-DOF vehicle longitudinal model is used for this simulation analysis. The vehicle longitudinal model developed by Aparow et al. (2013) is used as the leading vehicle to evaluate the performance of FCW using a two-wheeler bike model. The detailed derivation of the vehicle longitudinal is shown in Aparow et al. (2013) using the Pacejka Magic Tire model.

The vehicle longitudinal model of a passenger vehicle considered consists of a single sprung mass representing the vehicle body. This sprung mass is connected to four unsprung masses representing the wheels at the corners, thus representing a five-degree of freedom (5-DOF) system. The sprung mass is represented as a single plane and allows displacement in the longitudinal direction only (neglecting the lateral and vertical directions). Each of the wheels is allowed to rotate about its axis and all four wheels moved in longitudinal directions. The power train model and brake dynamics are included in this modeling as it contributes significantly to the performance of the vehicle model.

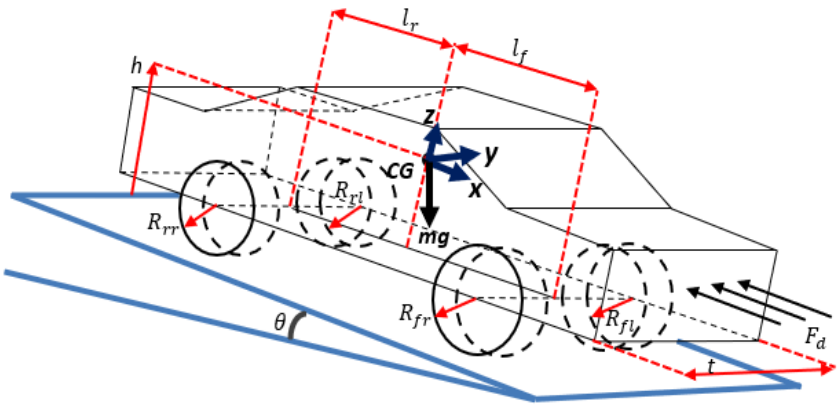

FIGURE 12: A 3D diagram of the vehicle's longitudinal model

4. CONTROL STRUCTURE USING BIKE LONGITUDINAL MODEL

The control structure for the Forward Collision Prevention (FCP) system can be developed using the bike model. The FCP algorithm is designed based on the FCW algorithm which was developed in previous work (Zhang et al., 2020). The choice of algorithm in this study will be the kinematic-based warning algorithm. The Berkeley-Algorithm which is the improved version of the Mazda algorithm can be considered a well-rounded algorithm for the FCP system. The output of the Berkeley algorithm is integrated with PID control for the throttle position and the brake input force of the bike. In such cases, the FCW system can be improved to a semi-ACC system for the bike, which is called the Forward Collision Prevention (FCP) system. In this study, a closed-loop control structure is used to regulate the throttle position and brakes of the vehicle with two independent PID controllers. The input for both PID control is the dimensionless warning value, ψ from equation (20) whereas the outputs of the controllers are brake input force and throttle. Both outputs will then be fed to the bike model.

4.1 Design of the Control Algorithm

This section will include the development of the control algorithm of the FCW system based on the Berkeley algorithm. Then, the control algorithm will be implemented with a PID controller for throttle control and brake control of the bike model to form a collision prevention system called as the Forward Collision Prevention (FCP) system.

4.1.1 Berkeley Algorithm

As discussed above, the Berkeley algorithm is modeled in SIMULINK based on equations (20) to (22) The velocity and distance data for both the bike and leading vehicle is the input of the algorithm. In real situations, the distance between the vehicle and the velocities for both vehicles can be obtained via a radar sensor. The maximum deceleration can be obtained via the speed sensors in the bike. The output of the algorithm is fed to the PID control block for both the brake and throttle. The risk of collision increases as the value of ψ increases; the risk of collision decreases as the value of ψ decreases; there is no risk of collision if the value of ψ is greater than 1. The maximum deceleration of the bike is 10 ms-2 and the total system delay and driver reaction time is 1.1 seconds. There is a 5m of minimum headway distance when the bike comes to a stop.

$$D_w = \frac{1}{2} * \left(\frac{v^2}{a_1} - \frac{(v - v_0)^2}{a_2} \right) + v(t_1 + t_2) + d_0 \quad (20)$$

$$\psi = \frac{d - D_w}{D_w - D_b} \quad (20)$$

$$D_b = v_0(t_1 + t_2) + \frac{1}{2} a(t_1 + t_2)^2 \quad (22)$$

Where d_0 = head offset distance,
v = subject vehicle speed,
v_0 = relative speed between vehicles,
t_1 = system delay,
t_2 = driver reaction time,
a_1 = maximum brake deceleration of the subject vehicle
a_2 = maximum brake deceleration of the leading vehicle.

4.1.2 PID Controller for Throttle

A Proportional-Integral-Derivative controller (PID) is a control loop mechanism to adjust an error rate close to the set point as described in equation (23). A closed-loop PID uses a feedback signal to compare the error rate with the set point value and make an adjustment based on the three parameters of the controller. Three constant parameters of the PID controller which are proportional (P), integral (I), and derivative (D) are optimized using Knowledge Based Tuning (KBT) method. Optimized parameters were used for the three-test case testing which will be explained in the next section.

$$u(t) = K_p e(t) + K_i \int e(t)dt + K_p \frac{de}{dt} \tag{23}$$

Implementation of the PID controller to the algorithm allows the Berkeley algorithm to control the throttle and brake in a more stable state as overshooting is not allowed for a moving bike. As mentioned above, a closed-loop PID system is developed, and the control system uses the bike model as a plant to be controlled. The output of the Berkeley algorithm is fed into the PID controller to control the throttle position of the bike. The error rate of velocity and braking distance is calculated by the Berkeley algorithm and the PID controller will adjust and corrections on the error rate to maintain a safe distance between the vehicle and adjust the velocity of the bike to match the leading vehicle velocity. The closed-loop PID control with the Berkeley algorithm is shown in Figure 13.

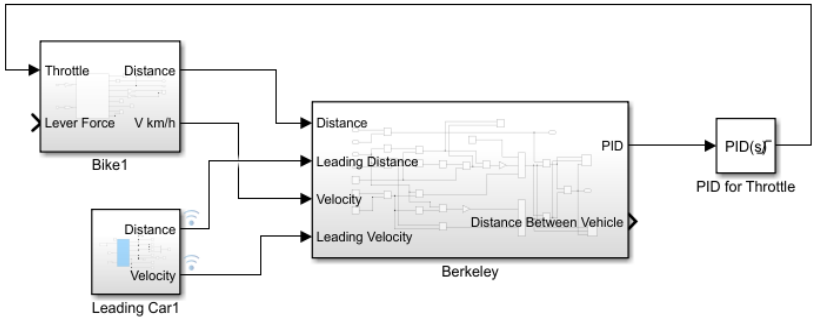

FIGURE 13: Close loop PID system for throttle

4.1.3 PID Controller for Brakes

The PID controller for the brake uses the same method of control as the throttle control. The risk of collision increases as the value of ψ increases; the risk of collision decreases as the value of ψ decreases; there is no risk of collision if the value of ψ is greater than 1. Therefore, an If and else condition is made to trigger the brakes at certain conditions. From Figure 14, the brakes PID block will be triggered ON if the value of ψ>0.75 & ψ <1. As the value of ψ<0.75, the risk of collision is quite low where the throttle control can make an adjustment on the velocity of the bike to maintain a safe distance. In such cases where the leading vehicle suddenly brakes and the value of ψ>0.75 & ψ <1, the risk of collision is considered high where the brakes play an important role to help lower the velocity and maintain a safe distance between the bike and the leading vehicle.

$$PID\ Brake\ Controller = \begin{cases} \text{if} & \psi > 0.75\ \&\ \psi < 1 & Collision\ Risk\ is\ high, Brake\ is\ ON \\ \text{if} & \psi < 0.75 & Collision\ Risk\ is\ low, Brake\ is\ OFF \\ \text{if} & \psi > 1 & Collision\ Risk\ is\ 0, Brake\ is\ OFF \end{cases} \tag{24}$$

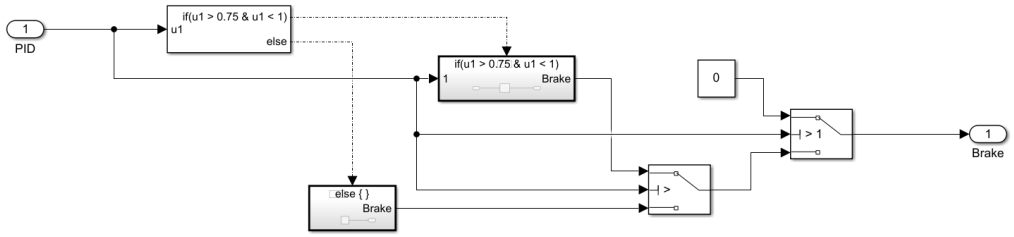

FIGURE 14: IF and ELSE conditions for the brake PID Controller

4.2 Configuration of the Forward Collision Prevention Control Algorithm for Bike Model

In this project, a car is used as the leading vehicle for the simulation. From Figure 15, the bike model throttle input is connected to a switch block. The bike will start from rest at t = 5s to t = 20s at 50% throttle then the PID controller will take over the throttle control.

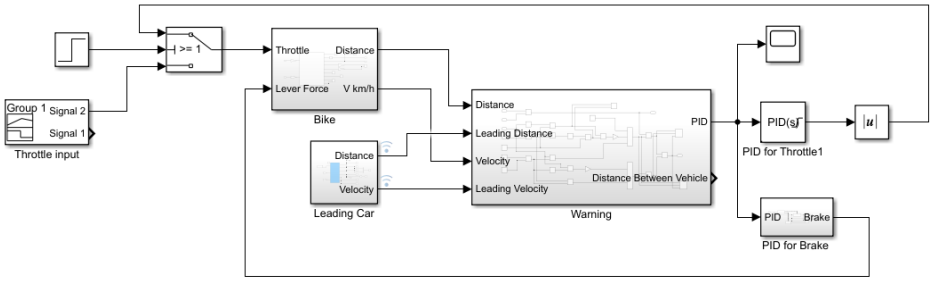

FIGURE 15: Forward Collision Prevention control algorithm

5. SIMULATION RESULTS

For every test case scenario, the bike will be at rest t = 0. At t = 5s, the bike accelerates at 50% throttle till t = 20s, then the PID controller will take over the throttle control for the bike model. Figure 16 shows the throttle profile for bikes at t = 0 to t = 20s. Each test case scenario will be simulated for 2,000 seconds.

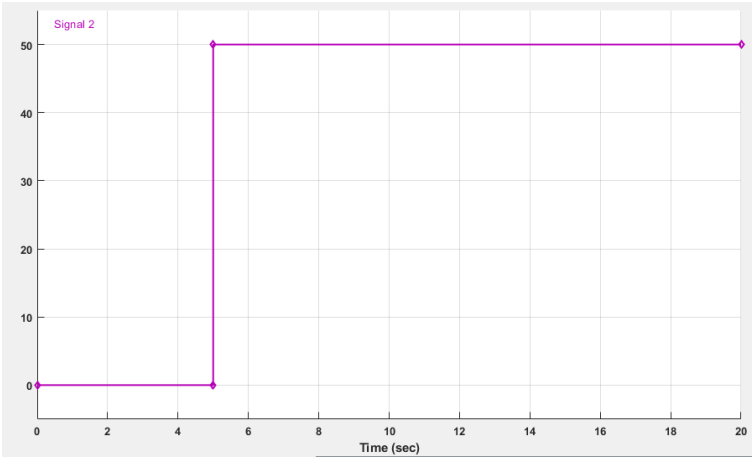

FIGURE 16: Throttle profile of the bike model at first 20 seconds

5.1 Test Case 1: Leading Vehicle Cruising at Constant Velocity

In this test case, the leading car accelerates from rest to a steady velocity of 34 km/h. The leading car will maintain its velocity till the end of the simulation. Figure 17 shows the throttle profile of the leading car. From Figure 18, it can be observed that both the leading vehicle and bike accelerate at a constant rate and the leading vehicle reaches a peak velocity of 45km/h and then slows down to 34km/h till the

end of the simulation. From the bike's perspective, it accelerates to reach the leading velocity profile as the distance between both vehicles is as far as 160 m apart. However, as the gap between the two vehicles reduces gradually the bike still accelerates further to reduce the gap. Based on Figure 18, at t = 200s the velocity of the bike exceeded the car until t = 1,200s. At t = 1,200s, the control algorithm PID controller successfully maintains the throttle level and brake level to keep a safe distance while maintaining the same velocity as the leading vehicle. The bike success to maintain a gap of 65m while following the cruising velocity of 34km/h. Based on Figure 21, the PID throttle level applies a full throttle at first then reduces the throttle level to 25% and maintains the throttle speed till t = 1,200s. Starting from t = 1,200s, the brake PID controller kicks in to help maintain the velocity and safety distance between both vehicles as the throttle controller alone cannot achieve that.

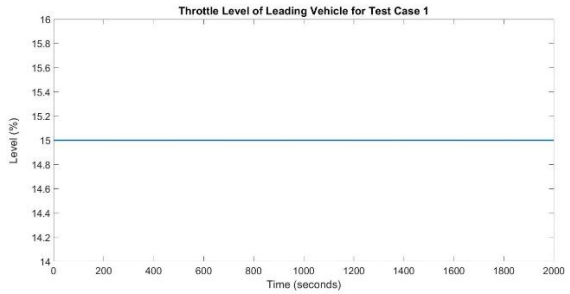

FIGURE 17: Throttle profile

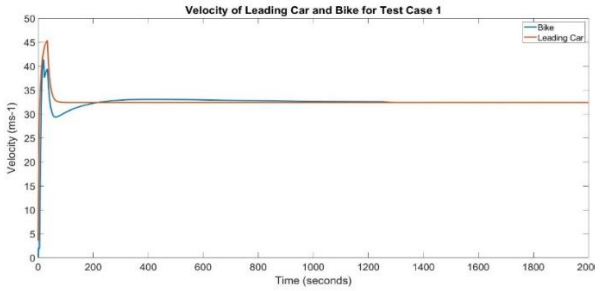

FIGURE 18: Velocity profile

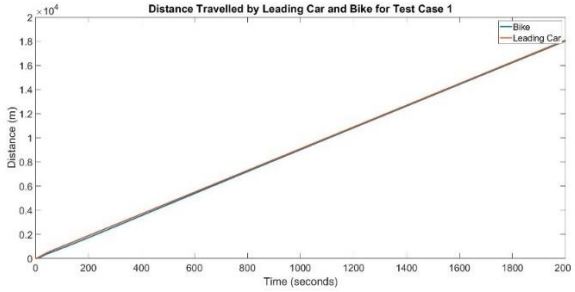

FIGURE 19: Distance travel

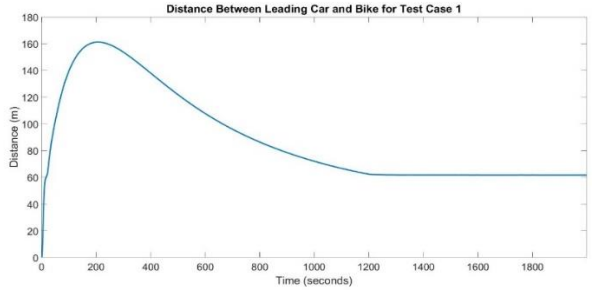

FIGURE 20: Absolute distance bet. bike & vehicle

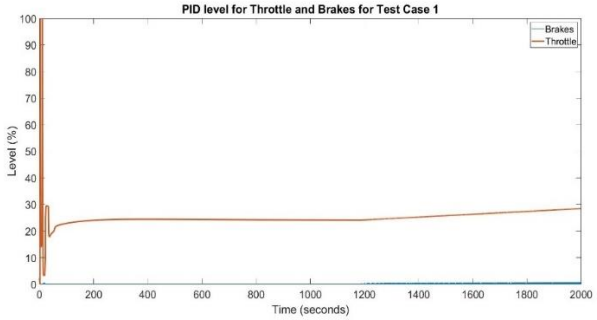

FIGURE 21: PID Control for Test Case 1

5.2 Test Case 2: Leading Vehicle Gradual Deceleration Profile

In this test case, the leading vehicle accelerates from rest with 50% throttle for 80 seconds. The leading vehicle then reduces the throttle to 25 % at t = 80s and maintains the same throttle input until t = 400s then reduced the throttle input to 15% at t = 400s. The leading vehicle then accelerates gradually to 25% throttle till t = 1,000s. Lastly, the leading vehicle slows down again to 20% throttle at the end of the simulation. The detail of the throttle profile for the leading vehicle is shown in Figure 22.

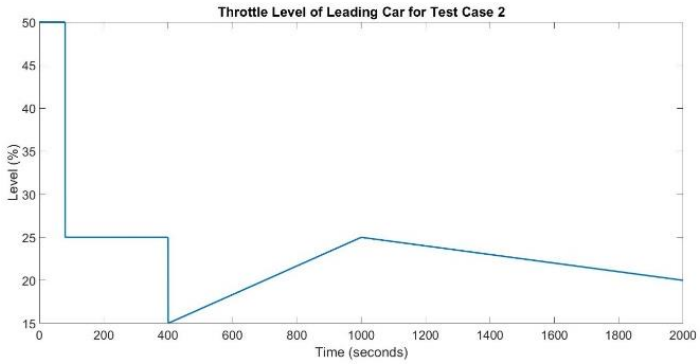

FIGURE 22: Throttle profile of the leading vehicle for Test Case 2

Figure 23 shows that the leading vehicle accelerates steadily and reaches the top velocity of 105km/h, at t = 80s the throttle for the leading car reduces to 25%. Hence, the velocity of the leading vehicle has been reduced and maintained at 85 km/h till t = 400s. At t = 400s, the velocity of the vehicle is reduced again as the throttle is lowered to 15%. The leading vehicle then gains velocity gradually at t = 600 till t = 1,100s and slows down steadily to 70km/h. For the bike, the PID controller again successfully follows the trend velocity of the leading vehicle while keeping a safe distance between both vehicles. From Figure 24, the leading vehicle leads the bike by 3250m. Hence, the PID controller set the maximum throttle for the bike to reach the leading vehicle's velocity. As the distance between vehicles reduces, the PID controller lowers the throttle value gradually to maintain a safe distance between the leading vehicle and the bike. Based on Figure 25, the bike successfully closes up the distance at t = 800m using PID controller input as shown in Figure 25, and is able to follow the velocity of the leading vehicle.

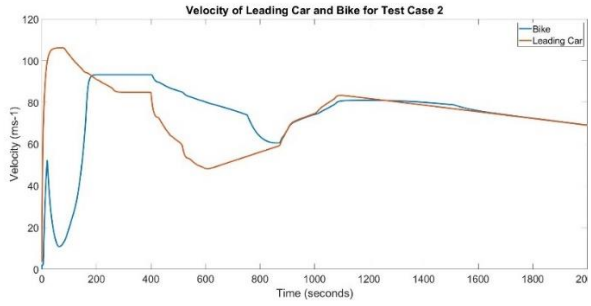

FIGURE 23: Velocity profile

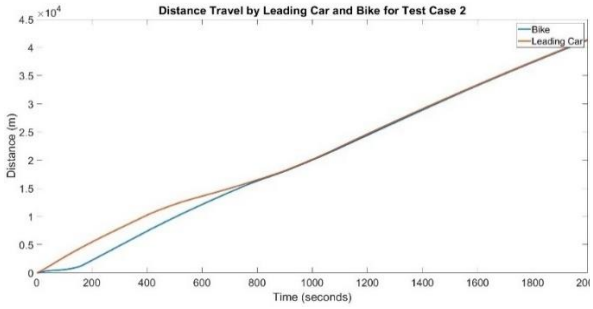

FIGURE 24: Distance travel

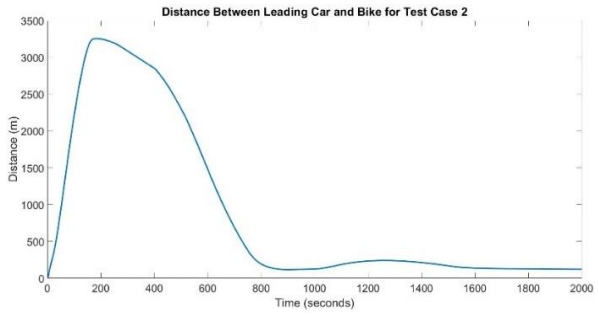

FIGURE 25: Absolute distance bet. bike & vehicle

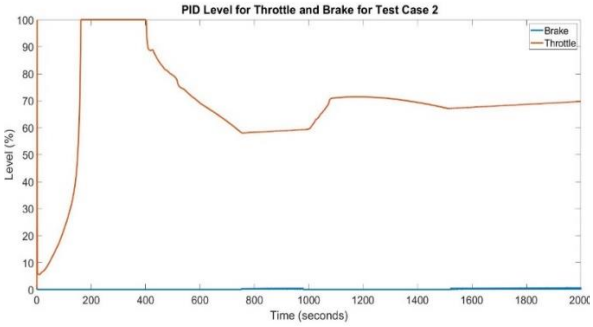

FIGURE 26: PID Control for Test Case 2

5.3 Test Case 3: Leading Vehicle Sudden Acceleration and Deceleration

In this test case, the leading vehicle accelerates from rest with 40% throttle from t = 0s to t = 400s. The leading vehicle then releases all the throttle to 0% and then increases the throttle by 20% at t = 600s. This test case allows us to simulate the condition where the leading vehicle suddenly slows down to a very low velocity. Figure 27 shows the throttle profile of the leading vehicle for the third test case.

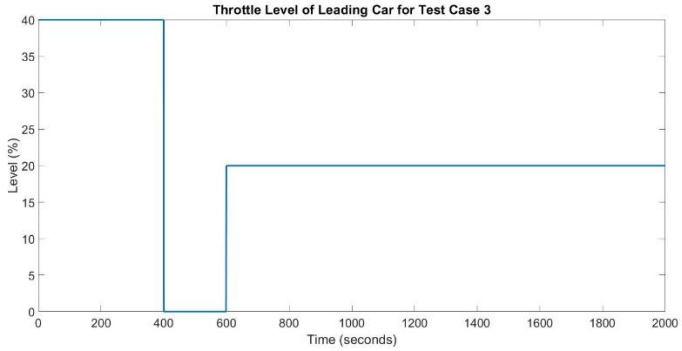

FIGURE 27: Throttle profile of the leading vehicle for Test Case 3

Based on Figure 28, the velocity of the leading car reaches a peak of 85km/h and drops to 5km/h at t = 400s. The car accelerates again at t = 600s to a steady 45km/h till the end of the simulation. As stated above, this test case simulated the sudden acceleration and deceleration conditions. The main purpose of this test case is to test the functionality of the PID controller to follow back the speed of the leading vehicle whenever the leading vehicle slows down significantly. From Figure 31, the PID controller passes the test and successfully follows the sudden acceleration and deceleration profile of the leading vehicle as the bike accelerates back to 45 km/h at t = 600s. From Figure 35, it can be observed that there is a delay in applying sudden braking for the bike when the leading vehicle slows down suddenly from 85 km/h to 5 km/h. However, the throttle controller can reduce the velocity of the bike where at t = 600s, the distance between both the leading vehicle and the bike is only 15m apart.

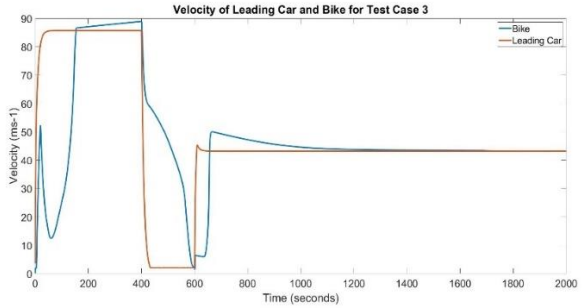

Figure 28: Velocity profile

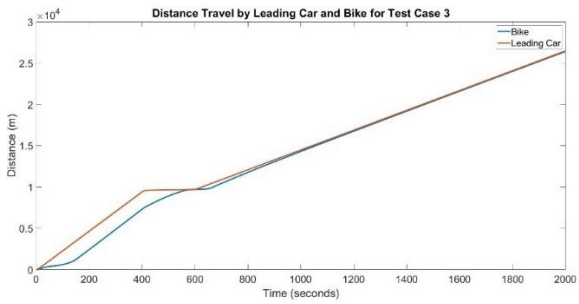

Figure 29: Distance travel

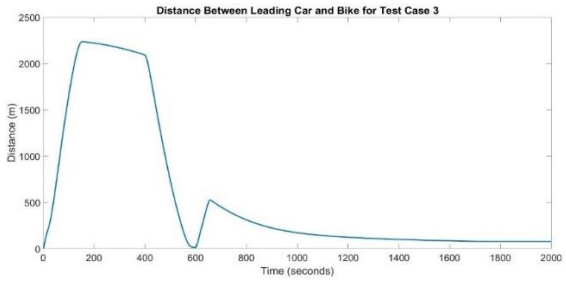

Figure 30: Absolute distance bet. bike & vehicle

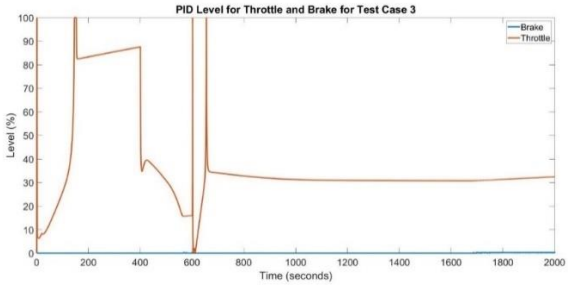

Figure 31: PID Control for Test Case 3

6. CONCLUSION

The main aim of this study is to ensure the bike can maintain a safe distance from the leading vehicle and follow the speed of the leading car. It can be observed that the developed control algorithm of the Forward Collision Prevention (FCP) system based on the Berkeley algorithm can control the throttle and brake level of the bike. The bike model is tested with three different scenarios with each scenario simulating different modes of driving patterns on road. Test Case 1 simulates the bike tailing a low cruising speed leading vehicle, Test Case 2 simulates the ability of the bike slows downs and speed up whenever the leading vehicle does so, and Test Case 3 simulates the sudden acceleration and

deceleration conditions. Overall, the control algorithm passes all three test cases and can achieve the objective of maintaining distance while following the cruising speed of the leading car at a minimum distance of 5m.

ACKNOWLEDGEMENT

This work is part of the research project entitled “Vehicle-in-the-loop safety testing platform for autonomous vehicles using Malaysian road and traffic environment”. This research is fully supported by Yayasan Tun Ismail Mohamed Ali Berdaftar (YTI) under the Permodalan Nasional Berhad (PNB), and the grant is led by Assistant Professor Dr. Vimal Rau Aparow. The authors would also like to thank the University of Nottingham Malaysia for its continuous support to conduct research in this area.

REFERENCES

Abdul Manan, M. M., Ho, J. S., Syed Tajul Arif, S. T. M., Abd Ghani, M. R., Ishak, S. Z., & Wong, S. V. (2018). Speed study and behaviour observation of motorcyclists along Malaysian roads (No. 248). MIROS Research Report, MRR.

Ahmad, F., Mazlan, S. A., Zamzuri, H., Jamaluddin, H., Hudha, K., & Short, M. (2014). Modelling and validation of the vehicle longitudinal model. International Journal of Automotive & Mechanical Engineering, 10.

Aparow, V. R., Ahmad, F., Hudha, K., & Jamaluddin, H. (2013). Modelling and PID control of Antilock Braking System with wheel slip reduction to improve braking performance. International Journal of Vehicle Safety, 6(3), 265-296.

Barbagallo, R., Sequenzia, G., Oliveri, S. M., & Cammarata, A. (2016). Dynamics of a high-performance motorcycle by an advanced multibody/control co-simulation. Proceedings of the Institution of Mechanical Engineers, Part K: Journal of Multi-body Dynamics, 230(2), 207-221.

Biral, F., Lot, R., Sartori, R., Borin, A., & Roessler, B. (2010). An intelligent frontal collision warning system for motorcycles. In Proceedings of the Bicycle and Motorcycle Dynamics 2010 Symposium. Delft.

Bloecher, H. L., Dickmann, J., & Andres, M. (2009). Automotive active safety & comfort functions using radar. In 2009 IEEE International Conference on Ultra-Wideband (pp. 490-494). IEEE.

Bonci, A., De Amicis, R., Longhi, S., & Lorenzoni, E. (2018). A smooth traction control design for two-wheeled electric vehicles. In 2018 14th IEEE/ASME International Conference on Mechatronic and Embedded Systems and Applications (MESA) (pp. 1-6). IEEE.

Bonci, A., De Amicis, R., Longhi, S., Lorenzoni, E., & Scala, G. A. (2016). A motorcycle enhanced model for active safety devices in intelligent transport systems. In 2016 12th IEEE/ASME International Conference on Mechatronic and Embedded Systems and Applications (MESA) (pp. 1-6).

Bonci, A., De Amicis, R., Longhi, S., Lorenzoni, E., & Scala, G. A. (2016). Motorcycle's lateral stability issues: Comparison of methods for dynamic modelling of roll angle. In 2016 20th International Conference on System Theory, Control and Computing (ICSTCC) (pp. 607-612). IEEE.

Bonci, A., De Amicis, R., Longhi, S., Lorenzoni, E., & Scala, G. A. (2017). A motorcycle’s analytical model describing the highside fall in panic situations. IFAC-PapersOnLine, 50(1), 15616-15621.

Bonci, A., De Amicis, R., Longhi, S., Scala, G. A., & Andreucci, A. (2016). Motorcycle lateral and longitudinal dynamic modeling in presence of tyre slip and rear traction. In 2016 21st International Conference on Methods and Models in Automation and Robotics (MMAR) (pp. 391-396). IEEE.

Chen, T., Liu, K., Wang, Z., Deng, G., & Chen, B. (2019). Vehicle forward collision warning algorithm based on road friction. Transportation Research Part D: Transport and Environment, 66, 49-57.

Chen, Y. L., Shen, K. Y., & Wang, S. C. (2013). Forward collision warning system considering both time-to-collision and safety braking distance. In 2013 IEEE 8th Conference on Industrial Electronics and Applications (ICIEA) (pp. 972-977). IEEE.

Cicchino, J. B. (2017). Effectiveness of forward collision warning and autonomous emergency braking systems in reducing front-to-rear crash rates. Accident Analysis & Prevention, 99, 142-152.

Dagan, E., Mano, O., Stein, G. P., & Shashua, A. (2004). Forward collision warning with a single camera. In IEEE Intelligent Vehicles Symposium, 2004 (pp. 37-42). IEEE.

Kusano, K. D., & Gabler, H. C. (2012). Safety benefits of forward collision warning, brake assist, and autonomous braking systems in rear-end collisions. IEEE Transactions on Intelligent Transportation Systems, 13(4), 1546-1555.

Milanés, V., Llorca, D. F., Villagrá, J., Pérez, J., Fernández, C., Parra, I., ... & Sotelo, M. A. (2012). Intelligent automatic overtaking system using vision for vehicle detection. Expert Systems with Applications, 39(3), 3362-3373.

MIROS (2018). MIROS Annual Report 2018. Malaysian Institute of Road Safety and Research.

Savino, G., Lot, R., Massaro, M., Rizzi, M., Symeonidis, I., Will, S., & Brown, J. (2020). Active safety systems for powered two-wheelers: A systematic review. Traffic Injury Prevention, 21(1), 78-86.

Sharp, R. S., Evangelou, S., & Limebeer, D. J. (2004). Advances in the modelling of motorcycle dynamics. Multibody System Dynamics, 12(3), 251-283.

Turner, P., & Higgins, L. (2013). Intelligent Transportation System (ITS) technologies for motorcycle crash prevention and injury mitigation. In International Motorcycle Safety Conference (IMSC).

Wang, X., Chen, M., Zhu, M., & Tremont, P. (2016). Development of a kinematic-based forward collision warning algorithm using an advanced driving simulator. IEEE Transactions on Intelligent Transportation Systems, 17(9), 2583-2591.

Zador, P. L., Krawchuk, S. A., & Voas, R. B. (2000). Automotive collision avoidance system (ACAS) program (No. DOT HS 809 080).

Zhang, K., Liu, W., Li, J., & Zhang, L. (2021). Stratified control strategy of vehicle longitudinal active collision avoidance. In Journal of Physics: Conference Series (Vol. 1735, No. 1, p. 012003). IOP Publishing.

Zhang, Y. J., Du, F., Wang, J., Ke, L. S., Wang, M., Hu, Y., ... & Zhan, A. Y. (2020). A safety collision avoidance algorithm based on comprehensive characteristics. Complexity, 2020.